# Pay More Attention to Discontinuity for Medical Image Segmentation

Jiajia Chu[1], Yajie Chen[1], Wei Zhou[1], Heshui Shi[2,3], Yukun Cao[2,3], Dandan Tu[4], Richu Jin[4], and Yongchao Xu[1(✉)]

[1] School of Electronic Information and Communications, Huazhong University of Science and Technology, Wuhan, China
yongchaoxu@hust.edu.cn
[2] Department of Radiology, Union Hospital, Tongji Medical College, Huazhong University of Science and Technology, Wuhan, China
[3] Hubei Province Key Laboratory of Molecular Imaging, Wuhan, China
[4] HUST-HW Joint Innovation Lab, Wuhan, China

**Abstract.** Medical image segmentation is one of the most important tasks for computer aided diagnosis in medical image analysis. Thanks to deep learning, great progress has been made recently. Yet, most existing segmentation methods still struggle at discontinuity positions (including region boundary and discontinuity within regions), especially when generalized to unseen datasets. In particular, discontinuity within regions and being close to the real region contours may cause wrong boundary delineation. In this paper, different from existing methods that focus only on alleviating the discontinuity issue on region boundary, we propose to pay more attention to all discontinuity including the discontinuity within regions. Specifically, we leverage a simple edge detector to locate all the discontinuity and apply additional supervision on these areas. Extensive experiments on cardiac, prostate, and liver segmentation tasks demonstrate that such a simple approach effectively mitigates the inaccurate segmentation due to discontinuity and achieves noticeable improvements over some state-of-the-art methods.

**Keywords:** Discontinuity · Medical image segmentation · Edge detection

## 1 Introduction

Medical image segmentation which extracts anatomy information is one of the most important tasks in medical image analysis. In recent years, great progress has been made thanks to the development of deep learning. Yet, it is still challenging to accurately delineate the region boundary between regions of interest, which is important in clinical usage.

Different from semantic segmentation of natural images that mainly focus on incorporating contextual information, state-of-the-art methods in medical image


A. L. Martel et al. (Eds.): MICCAI 2020, LNCS 12264, pp. 166–175, 2020.
https://doi.org/10.1007/978-3-030-59719-1_17

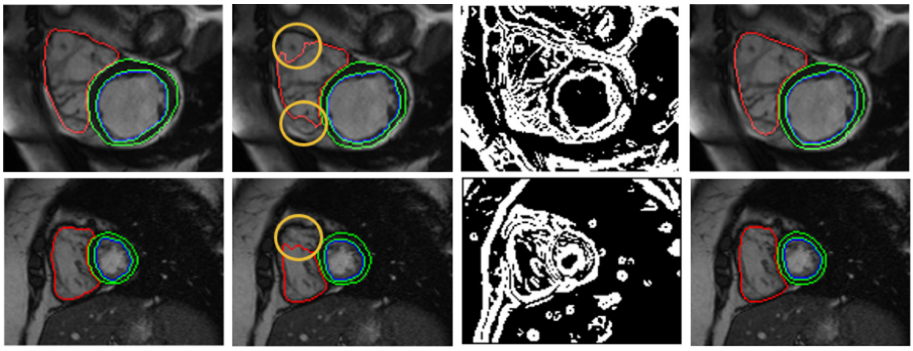

(a) GT (b) Baseline (c) Discontinuity (d) Ours

**Fig. 1.** Some segmentation examples. Top row: in-dataset validation. Bottom row: cross-dataset validation. By paying more attention to all discontinuity positions in (c) obtained with a simple edge detector, we can avoid the confusing delineation (see the yellow ellipses in (b)) caused by discontinuity within regions and being close to the region boundary, and thus achieve accurate segmentation in (d). (Color figure online)

segmentation put much effort in either improving the network design, incorporating the anatomical prior information, or developing dedicated loss functions, to improve the segmentation accuracy. They can be roughly categorized into these three classes.

For the methods that rely on novel network design, the U-net [1] is one of the most popular convolutional network architecture used in medical image segmentation. Some following methods [2–4] aim to improve the architecture of U-net and achieve boosted performance. Isensee *et al.* [5] proposed nnU-net (no-new-Net) [5] which can automatically design simple U-net and has achieved important improvement over the original U-net [1].

Medical images usually have some anatomical prior structure, based on which some methods [6,7] attempt to integrate such prior information to improve the segmentation accuracy. For example, Yue *et al.* [6] take into account the spatial information by predicting the spatial positions for each slice and regularizes the segmentation result into a desired realistic shape. In [7], the authors leverage an adversarial variational autoencoder to automatically correct the anatomically inaccurate shapes.

Some other methods focus on developing novel loss functions for medical image segmentation. Popular examples are Dice loss [2] and focal loss [8] which can mitigate the class imbalance problem faced by many medical image segmentation tasks. They result in improved accuracy but do not explicitly extract precise boundaries, which is crucial in clinical usage. In [9], Kervadec *et al.* proposed boundary loss that explicitly forces the boundary of segmentation result to align with the ground-truth region boundary. Chen *et al.* [10] developed a novel loss based on active contour models that also achieves accurate boundaries.

Despite much effort in improving the segmentation accuracy, it is still difficult to accurately delineate the region boundary. In practice, it is reasonable that a quasi-flat region may have similar segmentation output, and discontinuity positions may cause different segmentation outputs. Therefore, the discontinuity within regions may cause implausible boundary delineation. This discontinuity issue is more prominent for cross-dataset validation. Indeed, as depicted in Fig. 1, the discontinuity within regions and being close to the region boundary (see yellow ellipses) confuses the baseline model falsely regard such discontinuity positions as the region boundary, leading to inaccurate segmentation results.

In this paper, to address the discontinuity issue, we propose a simple yet effective approach by paying more attention to all discontinuity positions. Specifically, we first apply a simple edge detector to locate the discontinuity positions. Then in addition to the normal loss (*e.g.*, Dice loss [2]) on the whole image, we add an extra loss (*e.g.*, Dice loss [2]) on the discontinuity areas. Such a simple approach effectively alleviates the discontinuity issue and yields accurate boundary delineation (see for example Fig. 1). Extensive experiments on three medical image segmentation tasks (*i.e.*, cardiac, prostate, and liver segmentation) demonstrate the usefulness of the proposed approach.

The main contributions of this paper are three-folds: 1) In addition to region boundary which may pose problems for accurate medical image segmentation, to the best of our knowledge, we reveal for the first time that the discontinuity within regions can also cause inaccurate boundary delineation in medical image segmentation. 2) We propose a simple yet effective approach to alleviate such issue by simply paying more attention to the discontinuity obtained with a simple edge detector. 3) Without bells and whistles, the proposed method consistently achieves noticeable improvements over some related state-of-the-art methods on three medical image segmentation tasks.

## 2 Method

### 2.1 Motivation

Current mainstream medical segmentation methods are based on deep convolutional neural networks. They have achieved impressive performance in many segmentation tasks. Yet, the performance usually drops a lot when generalized to unseen datasets, which is the case in clinical usage. It is also crucial to accurately delineate the region boundaries, which usually correspond to some discontinuity positions. Indeed, we observe that quasi-flat regions usually have the same segmentation output, and areas around discontinuity positions are more likely to have different segmentation output. The discontinuity within regions and especially for those near the region contour can somehow confuse the segmentation model to make wrong boundary decision. Based on this finding, we propose to simply pay more attention to all discontinuity positions which may trigger inaccurate segmentation. The overall pipeline is depicted in Fig. 2. Hopefully, this will alleviate the problem of predicting some discontinuity positions within regions as the region boundary.

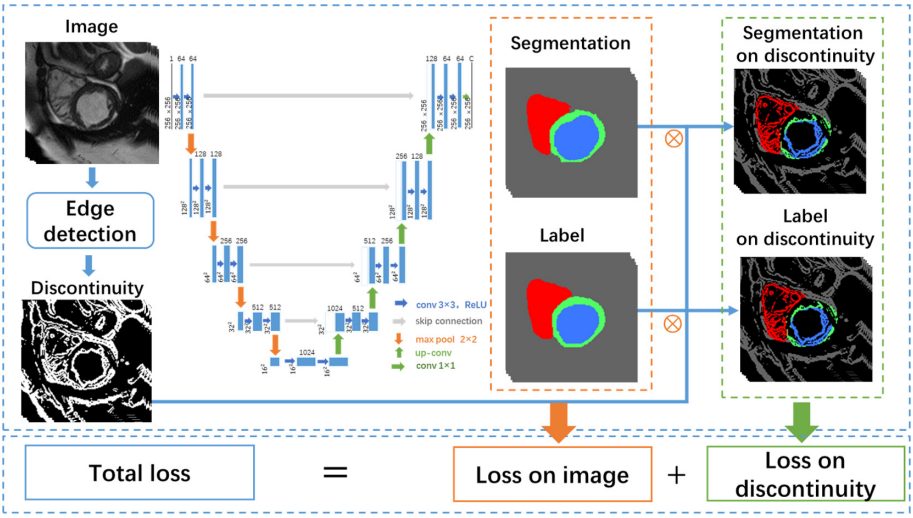


**Fig. 2.** Pipeline of the proposed method. We build the proposed approach on U-net baseline [1] by adding an additional loss on the discontinuity positions obtained by a simple edge detector.

### 2.2 Paying More Attention to Discontinuity

Most existing medical image segmentation methods apply cross-entropy loss or Dice loss [2] on the image domain $\Omega$. Specifically, The Dice loss [2] $L_d$ is less sensitive to class imbalance issue. It is given by:

$$L_d(\Omega) = 1 - \frac{1}{K}\sum_{c=1}^{K}\left(\frac{2\sum_{x\in\Omega} p_c(x) \times g_c(x)}{\sum_{x\in\Omega} p_c(x) + \sum_{x\in\Omega} g_c(x)}\right) \tag{1}$$

where $p_c(x)$ and $g_c(x)$ represent the probability of the pixel $x$ belonging to the class $c$ in prediction and ground truth, respectively.

In practice, we observe that discontinuity positions near the region boundary can be easily misclassified, resulting in boundary misalignment between segmentation result and ground truth segmentation. To mitigate such effect, we propose to pay more attention to all discontinuity positions. This is achieved by adding extra supervision on the discontinuity areas. Specifically, we first extract the discontinuity by applying a simple edge detector (*e.g.*., Scharr Filter [11]) on the image. We regard the top 25% edge responses in the image as the candidate discontinuity positions $\mathbb{D}$. Then we apply an additional Dice loss on the discontinuity areas $\mathbb{D}$. Therefore, the total loss is given by:

$$L = L_d(\Omega) + \lambda \times L_d(\mathbb{D}) \tag{2}$$

where $\lambda$ is a hyper-parameter which is set to 1 in all experiments.

### 2.3 Implementation Details

For the segmentation network, many different architectures have been used in medical image segmentation. The most popular and classic is U-net [1]. As noticed in nnU-net [5], many U-net alternatives slightly improve the original U-net. Therefore, though the proposed mechanism of paying more attention to discontinuity is suitable for any network architecture, we adopt the original U-net as our backbone network. More precisely, we employ U-net with 15 layers and batch normalization without dropout in all experiments. We optimize the network using Adam [12] with a learning rate set to 0.001, and resize all images to $256 \times 256$. All experiments are repeated three times and their average is considered as the final result.

## 3 Experiments

To demonstrate the effectiveness of the proposed method, we conduct experiments on three medical image segmentation tasks: cardiac, liver, and prostate segmentation.

### 3.1 Dataset and Evaluation Metrics

**Cardiac500 Dataset:** The Cardiac500 Dataset was collected by ourselves from a large hospital. It contains 531 patients divided into 5 subgroups: normal subjects, myocardial infarction, dilated cardiomyopathy, hypertrophic cardiomyopathy, and abnormal right ventricle. Each patient was collected at 25 time points, constructing a large-scale 4D cardiac dataset. Each case has 8–12 slices, and the whole dataset contains more than 100K 2D cardiac images. The right ventricles (RV), left ventricles (LV), and myocardium (Myo) are annotated by the cardiac physician. We divide the dataset into training set and test set according to the proportion of 8:2 in terms of patient level, resulting in 2645 test cases. All images are resized to $256 \times 256$. We train the network for 10 epochs on the training set and report results on the test set.

**ACDC Dataset:** The ACDC dataset [13] was acquired from two MRI scanners (1.5T and 3.0T) and used in the STACOM 2017 ACDC challenge[1]. It comprises 150 patients divided into the same 5 subgroups and annotated with the same three classes as the self-collected Cardiac500 dataset. The MRI data with associated annotations for 100 patients is publicly released, and the MRI data for the other 50 patients is released with their annotations hold by the challenge organizer. We leverage the MRI data for the 100 released patients with annotations for cross-dataset validation.

**Liver Segmentation:** The Liver dataset (T2-SPIR) is provided by the Combined Healthy Abdominal Organ Segmentation (CHAOS) Challenge in which

[1] https://www.creatis.insa-lyon.fr/Challenge/acdc/index.html.

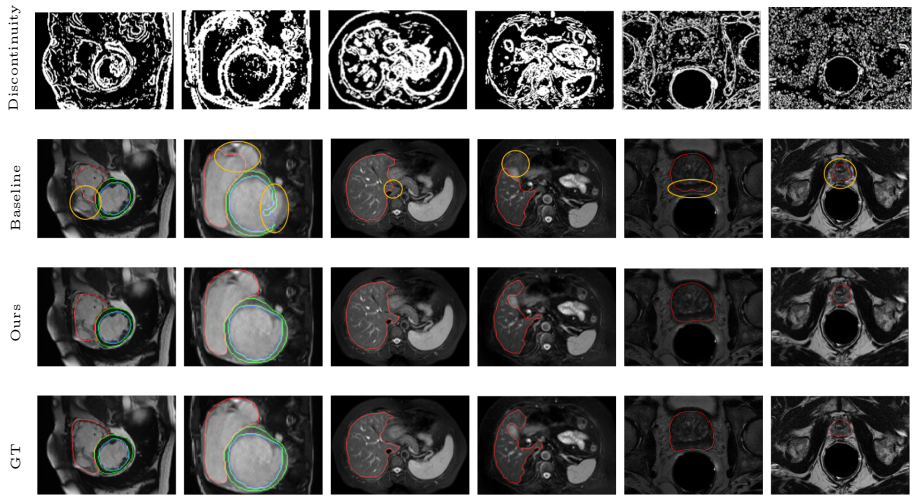


**Fig. 3.** Some qualitative illustrations. The discontinuity within regions and being close to the region boundary may be falsely regarded as the region boundary for the baseline method. By paying more attention to all discontinuity pixels (see the first row) obtained with a simple edge detector, the proposed method can alleviate such issue.

all images are acquired by a 1.5T Philips MRI and of size $256 \times 256$. CHAOS dataset contains 20 fully annotated subjects and 20 without annotation. We split the 20 fully annotated subjects into 15 for training and 5 for testing.

**Prostate Segmentation:** The Prostate dataset contains 40 patients from the PROSTATE-DIAGNOSIS collection [14] scanned with a 1.5T Philips Achieva MRI scanner. It is split into 30 patients for training, 5 for testing, and 5 for the competition (not used in our experiments). The labels are provided by Cancer Imaging Archive (TCIA) site [15]. The image size is $400 \times 400$ or $432 \times 432$. This dataset has two labeled categories, peripheral zone (PZ) and central gland (CG). Following [16], we consider both PZ and CG as the prostate region, and use 28 subjects with correct annotations to train the network and test on 5 test subjects.

**Evaluation Protocol:** We follow the common evaluation protocol relying on the 3D Dice coefficient.

### 3.2 Results

We compare the proposed method with the popular baseline U-net [1] with Dice loss, alternative (termed Boundary-enhanced loss) that applies larger loss weight on ground-truth region boundary, and two state-of-the-art methods that present novel loss functions: boundary loss [9] and active contour loss [10], on cardiac, liver, and prostate segmentation.

**Table 1.** Dice scores (%) of different methods on the self-collected Cardiac500 Dataset.

| Methods | RV | Myo | LV | Average |
|---|---|---|---|---|
| Baseline | 90.39 | 84.24 | 93.83 | 89.49 |
| Boundary loss [9] | 90.47 | 85.08 | 93.91 | 89.82 |
| Active contour loss [10] | **90.68** | 84.72 | 94.43 | 89.94 |
| Boundary-enhanced loss | 90.65 | 84.93 | 94.33 | 89.97 |
| Ours | 90.56 | **85.41** | **94.53** | **90.17** |

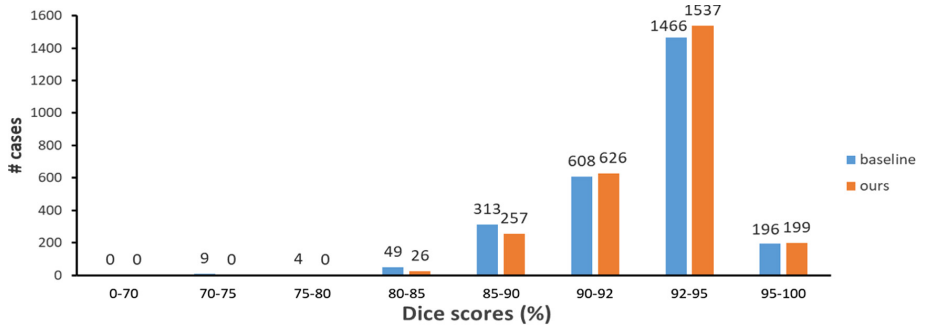


**Fig. 4.** Distribution of dice scores for 2645 cardiac cases in the self-collected Cardiac500 dataset. Compared with the baseline method, the proposed approach have more cases with Dice scores larger than 90%, and no cases ($VS$ 13 cases for the baseline method) with Dice scores smaller than 80%.

**Cardiac Segmentation.** We first conduct experiments on the large-scale self-collected Cardiac500 dataset. Some segmentation results are illustrated in Fig. 3 (left two columns). Qualitatively, the proposed approach mitigates the false boundary delineation on discontinuity within regions suffered by the baseline method, and thus achieves accurate segmentation results. The quantitative comparison with other methods is depicted in Table 1. Compared with the baseline method and the alternative by enhancing loss weights on ground-truth region boundary, paying more attention to discontinuity brings 0.68% and 0.2% Dice improvements. Since the self-collected Cardiac500 is a very large-scale dataset, such improvement over the baseline method is still noticeable. The proposed method also consistently improves boundary loss [9] and active contour loss [10] by 0.35% and 0.23% in terms of Dice score, respectively.

To further demonstrate the effectiveness of the proposed method, we also analyze the distribution of Dice scores for the proposed method and the baseline method. As shown in Fig. 4, the proposed method has 92 more images achieving Dice scores larger than 90% compared with the baseline, and there is no images ($VS$ 13 images for the baseline method) with Dice scores below 80%. This demonstrates the robustness of the proposed method in clinical usage.

**Table 2.** Cross-dataset validation in terms of Dice scores (%) for different methods trained on the self-collected Cardiac500 Dataset and tested on ACDC Dataset.

| Methods | RV | Myo | LV | Average |
|---|---|---|---|---|
| Baseline | 63.84 | 74.14 | 81.14 | 73.04 |
| Boundary loss [9] | 66.34 | 79.69 | 85.14 | 77.06 |
| Active contour loss [10] | 64.96 | 79.20 | 84.95 | 76.37 |
| Boundary-enhanced loss | 65.19 | 78.49 | 83.95 | 75.88 |
| Ours | **68.52** | **80.03** | **85.88** | **78.14** |

**Table 3.** Dice scores (%) of different methods on liver and prostate segmentation.

| Methods | Liver | Prostate |
|---|---|---|
| Baseline | 92.70 | 89.48 |
| Boundary loss [9] | 92.76 | 90.00 |
| Active contour loss [10] | 93.10 | 89.59 |
| Boundary-enhanced loss | 92.78 | 89.99 |
| Ours | **93.79** | **90.28** |

We then evaluate the proposed method and the competing methods under cross-dataset validation to further demonstrate the robustness of the proposed approach. As shown in Table 2, for the model trained on the large-scale self-collected Cardiac500 dataset, the proposed method outperforms all other methods when testing on the ACDC dataset [13]. Specifically, the proposed method achieves a Dice score of 78.14%, improving the baseline method and the alternative that enhances the loss weights on ground-truth region boundary by 5.1% and 2.26%, respectively. Compared with the boundary loss [9] and the active contour loss [10], the proposed method yields a Dice improvement of 1.08% and 1.77%, respectively.

**Liver Segmentation.** To further evaluate the effectiveness of the proposed method, next, we conduct experiments on liver segmentation. Some qualitative illustrations are shown in Fig. 3 (two columns in the middle). The same observation as on the cardiac segmentation also holds on liver segmentation. The quantitative comparison is depicted in Table 3. Similar to the result on cardiac segmentation, the proposed method outperforms all other methods in terms of Dice score. Precisely, the proposed method gives 1.09% and 1.01% Dice improvement over the baseline method and the alternative one, respectively. Compared with boundary loss [9] and active contour loss [10], the proposed method brings 1.03% and 0.69% Dice improvement, respectively.

**Prostate Segmentation.** We then conduct experiments on prostate (including peripheral zone (PZ) and central gland (CG)) segmentation. We show some qualitative results in the right two columns of Fig. 3. The proposed method aligns the ground-truth boundary better. The quantitative comparison is given in Table 3. The proposed method also consistently outperforms all other methods.

## 4 Conclusion

In this paper, we first reveal that the discontinuity within regions especially those near the region boundary may confuse the segmentation model in deducing accurate region boundary. Based on this observation, we propose a simple yet effective approach to alleviate such effects. Specifically, we propose to simply pay more attention to all discontinuity positions obtained by an edge detector. This is achieved by applying an additional loss on the discontinuity areas to supervise the network training. Despite its simplicity, we consistently achieve noticeable improvements over some state-of-the-art methods on three medical image segmentation tasks. The proposed method makes the segmentation more robust without requiring extra runtime. It is noteworthy that the proposed method is only beneficial for segmenting regions with discontinuity inside, and does not bring performance when the discontinuity within regions is not severe.

**Acknowledgement.** This work was supported in part by the Major Project for New Generation of AI under Grant no. 2018AAA0100400, NSFC 61703171, and NSF of Hubei Province of China under Grant 2018CFB199. Dr. Yongchao Xu was supported by the Young Elite Scientists Sponsorship Program by CAST.

## References

1. Ronneberger, O., Fischer, P., Brox, T.: U-Net: convolutional networks for biomedical image segmentation. In: Navab, N., Hornegger, J., Wells, W.M., Frangi, A.F. (eds.) MICCAI 2015. LNCS, vol. 9351, pp. 234–241. Springer, Cham (2015). https://doi.org/10.1007/978-3-319-24574-4_28
2. Milletari, F., Navab, N., Ahmadi, S.-A.: V-net: Fully convolutional neural networks for volumetric medical image segmentation. In: Proceedings of International Conference on 3D Vision, pp. 565–571 (2016)
3. Jegou, S., Drozdzal, M., Vazquez, D., Romero, A., Bengio, Y.: The one hundred layers tiramisu: fully convolutional DenseNets for semantic segmentation. In: Proceedings of IEEE International Conference on Computer Vision and Pattern Recognition, pp. 1175–1183 (2017)
4. Oktay, O., et al.: Attention u-net: Learning where to look for the pancreas. In: Proceedings of International Conference on Medical Imaging with Deep Learning (2018)
5. Isensee, F., et al.: NNU-Net: self-adapting framework for u-net-based medical image segmentation. arXiv preprint arXiv:1809.10486 (2018)
6. Yue, Q., Luo, X., Ye, Q., Xu, L., Zhuang, X.: Cardiac segmentation from LGE MRI using deep neural network incorporating shape and spatial priors. In: Shen, D., et al. (eds.) MICCAI 2019. Lecture Notes in Computer Science, vol. 11765, pp. 559–567. Springer, Cham (2019). https://doi.org/10.1007/978-3-030-32245-8_62

7. Painchaud, N., Skandarani, Y., Judge, T., Bernard, O., Lalande, A., Jodoin, P.-M.: Cardiac MRI segmentation with strong anatomical guarantees. In: Shen, D., et al. (eds.) MICCAI 2019. LNCS, vol. 11765, pp. 632–640. Springer, Cham (2019). https://doi.org/10.1007/978-3-030-32245-8_70
8. Lin, T.-Y., Goyal, P., Girshick, R., He, K., Dollàr, P.: Focal loss for dense object detection. IEEE Trans. Pattern Anal. Mach. Intell. **42**(2), 318–327 (2018)
9. Kervadec, H., Bouchtiba, J., Desrosiers, C., Granger, E., Dolz, J., Ayed, I.B.: Boundary loss for highly unbalanced segmentation. In: Proceedings of International Conference on Medical Imaging with Deep Learning, pp. 285–296 (2019)
10. Chen, X., Williams, B.M., Vallabhaneni, S.R., Czanner, G., Williams, R., Zheng, Y.: Learning active contour models for medical image segmentation. In: Proceedings of IEEE International Conference on Computer Vision and Pattern Recognition, pp. 11632–11640 (2019)
11. Jähne, B., Scharr, H., Körkel, S.: Principles of filter design. In: Handbook of Computer Vision and Applications, vol. 2, pp. 125–151 (1999)
12. Kingma, D.P., Ba, J.: Adam: a method for stochastic optimization. arXiv preprint arXiv:1412.6980 (2014)
13. Bernard, O., et al.: Deep learning techniques for automatic MRI cardiac multi-structures segmentation and diagnosis: is the problem solved? IEEE Trans. Med. Imaging **37**(11), 2514–2525 (2018)
14. Bloch, B.N., Jain, A., Jaffe, C.C.: Data from prostate-diagnosis. The Cancer Imaging Archive, 9 (2015). 10.7937K
15. Bloch, N., et al.: NCI-ISBI: challenge: automated segmentation of prostate structures. The Cancer Imaging Archive 370, 2015 (2013)
16. Liu, Q., Dou, Q., Yu, L., Heng, P.A.: MS-net: multi-site network for improving prostate segmentation with heterogeneous MRI data. IEEE Trans. Med. Imaging (2020)